ISSN 0021-3640, JETP Letters. ©The Authors(s), 2025. This article is an open access publication.

Computational Identification of Four Promising Nonlinear Optical Materials for Near and Middle Ultraviolet Operation

Y. Alkabakibi[+1)], *D. D. Barma*[+1)], *D. V. Rybkovskiy*[+1)], *A. Tudi*[*×], *C. Xie*[*×], *A. R. Oganov*[+1)]

[+]*Skolkovo Institute of Science and Technology, 121205 Moscow, Russian Federation*

[*]*Research Center for Crystal Materials, State Key Laboratory of Functional Materials and Devices for Special Environmental Conditions, Xinjiang Key Laboratory of Functional Crystal Materials, Xinjiang Technical Institute of Physics and Chemistry, CAS, 40-1 South Beijing Road, 830011 Urumqi, China*

[×]*Center of Materials Science and Optoelectronics Engineering, University of Chinese Academy of Sciences, 100049 Beijing, China*

Submitted 5 December 2024
Resubmitted 13 December 2024
Accepted 13 December 2024

We perform a computational search for promising nonlinear optical materials by screening crystal structure databases. We selected non-centrosymmetric, thermodynamically stable and low-energy metastable borates, with large expected band gaps. For these structures, we performed density functional computations of the gap values, birefringence and nonlinear susceptibilities. Our search revealed four potentially efficient nonlinear borate materials with large band gaps, moderate birefringence and high nonlinear coefficients: $K_3B_6O_{10}Cl$, $Ca_5B_3O_9F$, SrB_4O_7, $Al_4(B_2O_5)_3$.

DOI: 10.1134/S0021364024605074

Introduction. With the development of laser technologies, novel nonlinear optical (NLO) effects were discovered [1] and some of them were further employed for the design of promising devices. For instance, second harmonic generation (SHG) allows changing the radiation frequency. In many cases, this effect is used to obtain laser radiation of good quality at a wavelength for which a stable high-quality source simply does not exist.

Although nonlinear optical materials have been studied since the 1960s, there are only several practical materials like $KBe_2BO_3F_2$ (KBBF) that is used as active media in laser devices for laser generation in the deep ultraviolet (DUV) spectrum range (effective nonlinear coefficient $d_{\text{eff}} = 0.49$, birefringence $\Delta n = 0.08$, absorption edge $\lambda_{\text{cut off}} = 150\,\text{nm}$) [2–4] and KH_2PO_4 (KDP) – one of the oldest nonlinear materials whose properties are widely used as a reference for comparison ($d_{\text{eff}} = 0.384\,\text{pm/V}$, $\Delta n = 0.033$, $\lambda_{\text{cut off}} = 200\,\text{nm}$). The issue is that the UV (and especially deep UV, for short DUV) nonlinear materials must simultaneously meet the requirements for relatively high second-order susceptibility, DUV transparency, and high enough birefringence for phase matching [5]. To be transparent in the DUV region the material should have a wide band gap. At the same time the relation between the value of band gap and refractive index is inverse. And according to Miller's Rule the nonlinear susceptibility coefficient is proportional to $(n^2 - 1)^3$ [6]. This makes the search for nonlinear materials for the DUV spectral range challenging.

In crystals with favorable NLO-active structural units, which appear in high density and optimal mutual alignment, a combination of large NLO coefficients and birefringence can be achieved. There are different groups of crystals that exhibit their properties in the ultraviolet wavelength range. The most famous group of DUV nonlinear materials are borates, especially BPO_4, and phosphate crystals that are well-investigated and show excellent performance as NLO crystals [7]. Among them Bi_3TeBO_9 (BTBO) is a crystal with the strongest SHG response equal to 20× KDP [8, 9]. Also, the largest birefringence value for DUV transparent materials was found among borates: $Ca(BO_2)_2$ crystal possesses the birefringence value of 0.124 [10]. Frequently used $KBe_2BO_3F_2$ (KBBF) crystal can directly generate laser light with wavelength shorter than 200 nm by second harmonic generation (SHG), despite the fact that its further industrial applications are severely constrained by a few drawbacks: it contains highly toxic beryllium and it is difficult to grow its large crystals due to the platelet-like shape of the crystals, in addi-

[1)]e-mail: yomn.alkabakibi@skoltech.ru; daria.barma@skoltech.ru; d.rybkovskiy@skoltech.ru; a.oganov@skoltech.ru

tion to the existence of many polytypes which also negatively contributes to KBBF's NLO properties [11]. This structure has an effective nonlinear optical coefficient of 0.49 pm/V (about 1.3× KDP) and birefringence equal to 0.08 [2–4].

Other interesting groups of materials include fluorooxoborates and fluorophosphates, they show promising properties in terms of polarizability anisotropy, hyperpolarizability, and band gap, but often there is a problem with growing them as a bulky crystal. Compared to borates, partial substitution of O with F atoms reduces the symmetry and thus improves the ability to achieve a non-centrosymmetric phase [12].

Alternatives, such as carbonates and nitrates have also attracted researchers' attention in recent years, because they exclusively consist of π-conjugated groups [13]. This group of crystals shows high SHG efficiency (up to 3.5× KDP), but have phase-matching (PM) wavelengths close to 200 nm, which hinders their application in the DUV region.

Additionally, PN_2O_2 tetrahedron [14] as an active NLO unit was discovered recently. Using USPEX code two structures were predicted, one stable and one low-energy metastable. Both predicted structures have relatively wide band gaps greater than 6.2 eV, large birefringence (> 0.151 at 1064 nm) and SHG coefficients (about 6–9 times that of KDP).

Many borates have not been studied in terms of their nonlinear properties [15–17], but may be excellent candidates for the use in ultraviolet solid-state lasers. In this work we perform a computational search of promising NLO materials among the borates by screening existing crystal databases and performing density-functional computations of their NLO properties.

Computational methods. The investigation of the optical properties of borate materials was performed in frames of the density-functional theory (DFT) using the projector augmented wave (PAW) formalism [18] as implemented in the VASP software [19, 20]. Structural relaxation was carried out with use of the Perdew–Burke–Ernzerhof (PBE) [21] exchange-correlation functional. The cutoff energy of 600 eV was used for the expansion of the electronic wave functions. The k point grids with reciprocal-space resolution of $2\pi \times 0.04\,\text{Å}^{-1}$ were used for Brillouin zone sampling. Cell parameters and ionic positions were optimized with the conjugated-gradient algorithm until the forces were converged to 10 meV/Å.

After geometry optimization, the band gaps E_g, birefringence Δn and second order susceptibility tensors $\chi^{(2)}_{ijk}$ were calculated. Since the PBE functional is known to underestimate the band gaps, the Heyd–Scuseria–Ernzerhof (HSE06) [22] hybrid functional was used to obtain the E_g values.

Birefringence was calculated for the wavelength of 1064 nm, which is commonly employed in various optical applications. For doing this, the frequency-dependent dielectric tensor was calculated within the independent-particle approximation from the electronic band structure [23]. The dielectric tensor was diagonalized when required and the refractive indices were computed. Birefringence was obtained as the difference between the largest and smallest refractive indices.

Second-order susceptibility tensors $\chi^{(2)}_{ijk}$ were calculated within the independent-particle approximation. The method used in this work to calculate $\chi^{(2)}_{ijk}$ was first developed in [24], and then further modified and discussed by [25], where calculations on GaAs, GaP, and wurtzite GaN and AlN have shown excellent agreement with other ab initio methods. Moreover, further discussion of the accuracy of this method against experimental results was conducted in [26]. A scissor shift has been applied to the band gap according to the above mentioned HSE06 results. Since the computation of optical properties requires a denser k point grid, the smaller k point spacing of $2\pi \times 0.02\,\text{Å}^{-1}$ was used at this step. The number of conduction bands was set to be ~ 5 times higher than the number of valence bands.

Results and discussion. The identification of novel NLO borates was based on the screening of 2 crystal structure databases for structures with a combination of high nonlinear optical response, high birefringence, which is essential for phase matching, and a wide band gap, ensuring transparency within their operational UV wavelength range. We screened the Materials Project Database (MP) [27] and The Open Quantum Materials Database (OQMD) [28, 29] for crystals of 3 or 4 elements focusing on borates of Li, Na, K, Rb, Cs, Be, Mg, Ca, Sr, Ba, Al, Sc, Y or La, and allowing extra anions of F, N, Cl or I. The materials had to fulfil a set of conditions: we searched for non-centrosymmetric, thermodynamically stable and metastable structures with the energy not more than 10 me/atom above the convex hull, with expected band gap value more than 6 eV. Given the systematic underestimation associated with the PBE functional used in the Materials Project database, we included structures with calculated E_g values greater than 4 eV, to account for this underestimation.

The described filtering criteria were applied, resulted in a selection of 33 potentially promising candidates from the MP database and another 33 potentially promising candidates from the OQMD database. We then excluded structures that has been well investi-

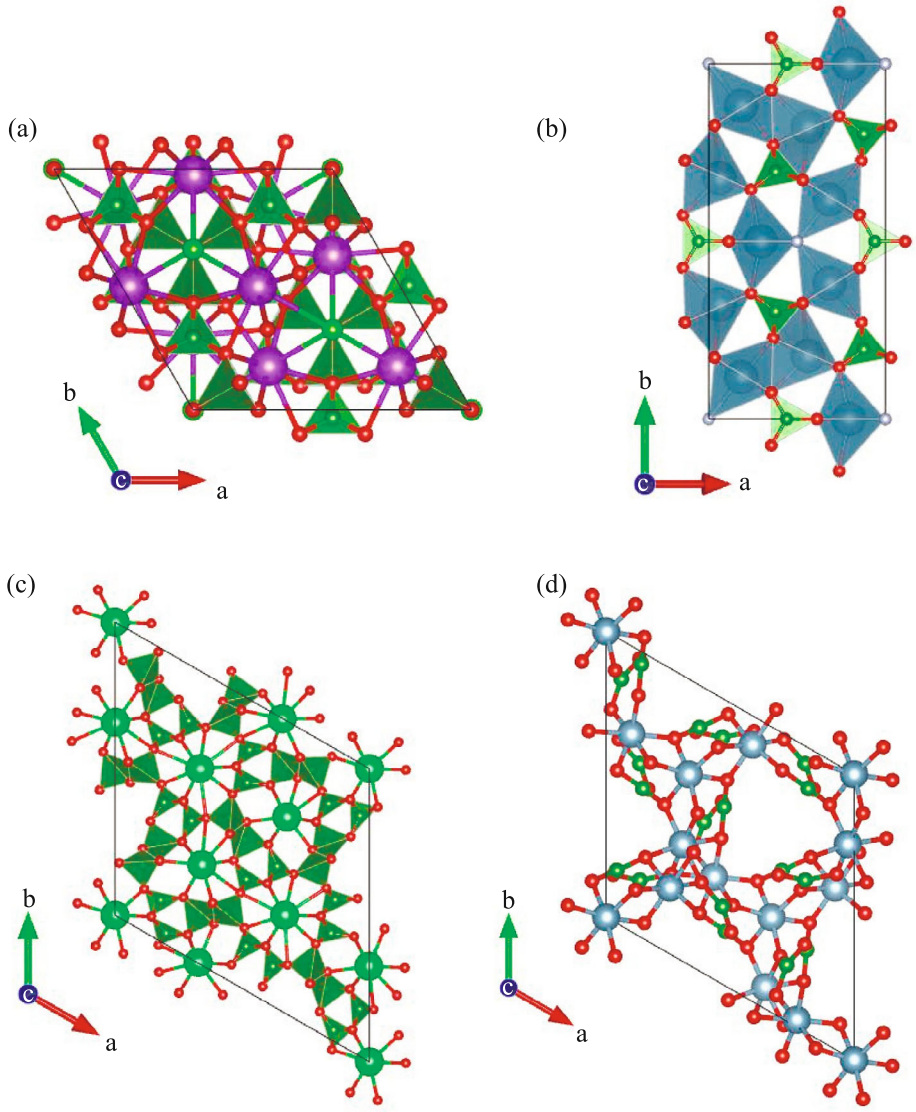

Fig. 1. (Color online) Crystal structures of (a) – $K_3B_6O_{10}Cl$, (b) – $Ca_5B_3O_9F$, (c) – SrB_4O_7, and (d) – $Al_4(B_2O_5)_3$, along c-axis. B and O atoms are illustrated by small green and red spheres in all structures, respectively. K and Cl are shown by violet and light-green in (a). Big and small grey spheres represent Ca and F in (b), respectively. Sr is shown by large light-green spheres in (c). Al is shown in grey in (d)

gated for their NLO properties, such as CsB_3O_5 (CBO), $Ba(BO_2)_2$ (BBO), LiB_3O_5 (LBO), Be_2BO_3F (BBF), $Sr_3B_6O_{11}F_2$ и Al_5BO_9, among others.

For the rest of candidate structures, we performed density-functional computations of linear and nonlinear optical properties as described in the methods section and revealed 4 promising NLO borate materials: $K_3B_6O_{10}Cl$, $Ca_5B_3O_9F$, SrB_4O_7 and $Al_4(B_2O_5)_3$. Their crystal structures are shown in Fig. 1.

$K_3B_6O_{10}Cl$ (KBOC) crystallizes in the noncentrosymmetric polar rhombohedral space group $R3m$. The crystal structure comprises hexaborate $[B_6O_{10}]$ units and $[ClK_6]$ octahedra. The hexaborate units consist of three BO_4 tetrahedra connected via shared oxygen vertices and three BO_3 triangles. Experimental studies conducted by Wu et al. revealed that KBOC powder samples exhibit a SHG efficiency that is four times higher than that of KDP. The greatest contribution to the nonlinear effect is formed due to BO_3 and BO_4 nonlinear units. The structure also has a desired low cutoff wavelength equal to 180 nm [30]. However, there have been no publications indicating the exact values of the components of the nonlinear susceptibility tensor.

$Ca_5(BO_3)_3F$ crystallizes in the monoclinic Cm space group. The structure features CaO_5F octahedra, where

Table 1. Structural information, band gap values E_g, calculated at the PBE and HSE06 levels of theory, absorption edge, birefringence Δn and phase-matching wavelength λ_{PM}

Chemical composition	Space group	Cell parameters (optimized at PBE level)	Cell volume	E_g (PBE), eV	E_g (HSE06), eV	Absorption edge, nm	Δn	λ_{PM}, nm
$K_3B_6O_{10}Cl$	$R3m$	$a = 10.16$ Å $c = 9.07$ Å	810.5 Å^3	5.38	6.76	184	0.049	310
$Ca_5B_3O_9F$	Cm	$a = 8.19$ Å $b = 16.22$ Å $c = 3.57$ Å $\beta = 79.23°$	466.2 Å^3	4.25	5.94	209	0.048	475
SrB_4O_7	$P3$	$a = 17.31$ Å $c = 4.29$ Å	1112.2 Å^3	5.17	6.80	182	0.043	355
$Al_4(B_2O_5)_3$	$R3$	$a = 11.58$ Å $c = 6.53$ Å	757.6 Å^3	5.81	7.57	164	0.047	290

each Ca^{2+} ion is coordinated by five O^{2-} ions and one F^- ion, forming a network of edge- and corner-sharing polyhedra. Additionally, the structure contains BO_3 units, which play a significant role in enabling the SHG effect. This compound has been examined both experimentally and theoretically in studies by Fletcher and Lei [31, 32]. However, its optical properties including the SHG tensor have not been investigated before.

SrB_4O_7 crystallizes in the trigonal $P3$ space group. BO_3 triangles and BO_4 tetrahedra are arranged in a 1:1 ratio on this structure. Both mentioned units will affect the second harmonic response. Compared with the other known polymorph of the same compound, α-SrB_4O_7, this trigonal phase has two types of nonlinear active units instead of one, which may lead to higher SHG response. The α-SrB_4O_7 phase is 0.007 eV/atom above the convex hull and has shown impressively low optical absorption edge (~ 130 nm) and high nonlinear coefficient [33, 34]. β-SrB_4O_7 studied here has a 0.002 eV/atom higher energy, and both these phases have been observed experimentally. For the purpose of this study, we calculated the SHG tensor and the birefringence of both phases. *Ab initio* calculations for α-SrB_4O_7 showed two times higher value of the SHG tensor's maximum component compared to β-SrB_4O_7, however, α-SrB_4O_7 exhibits low birefringence of 0.0038 making it unsuitable for NLO applications.

$Al_4B_6O_{15}$ crystallizes in the trigonal $R3$ space group. The structure consists of edge-sharing AlO_6 octahedra and the diborate B_2O_5 unit, where the two boron atoms are all triangularly coordinated by oxygen atoms. Borate groups and Al octahedral framework share oxygens, resulting in two types of three-membered ring units: one octahedron and two triangles and two octahedrons and one triangle [35]. The calculation of the second harmonic response of this material by means of a different approach (density-functional perturbation theory) was described in [36]. The *ab initio* method which we use in this study to calculate SHG tensor, is different and results in lower (likely more correct) values of SHG tensor components, due to the effect of the scissor operator.

The calculated band gap, absorption edge, birefringence and phase-matching wavelength values of the 4 structures are presented in Table 1, along with a summary of their chemical compositions, space groups and unit cell parameters.

Phase matching wavelengths were evaluated from the frequency dependences of refractive index eigenvalues. For example, for generating laser in the DUV range a material should have phase matching wavelength $\lambda_{PM} < 200$ nm, in addition to the absorption edge $\lambda_{\text{cutoff}} < 200$ nm and large SHG tensor components $d_{ij} > 0.38$ pm/V. Our results suggest that all four compounds should be very efficient in near UV ($Ca_5B_3O_9F$ and SrB_4O_7) and middle UV ($K_3B_6O_{10}Cl$ and $Al_4(B_2O_5)_3$) ranges.

After the calculation of electronic bands, birefringence, absorption edge and PM wavelength, the nonlinear susceptibility tensors $\chi^{(2)}_{ijk}$ were computed. In the literature on nonlinear optics, however, a more common quantity is the matrix of nonlinear coefficients, that are defined as $d_{ijk} = \frac{1}{2}\chi^{(2)}_{ijk}$. The calculated coefficients d, in units of pm/V, written in Voigt notation are:

$$d_{Ca_5B_3O_9F} =$$

$$\begin{bmatrix} 0.000 & 0.000 & 0.000 & 0.000 & -0.027 & 0.919 \\ 0.919 & -0.919 & 0.000 & -0.027 & 0.000 & 0.000 \\ -0.027 & -0.027 & 0.437 & 0.000 & 0.000 & 0.000 \end{bmatrix},$$

$$d_{Ca_5B_3O_9F} =$$

$$\begin{bmatrix} 0.218 & -0.701 & 0.100 & 0.000 & 0.474 & 0.000 \\ 0.000 & 0.000 & 0.000 & -0.507 & 0.000 & -0.701 \\ 0.474 & -0.507 & -0.013 & 0.000 & 0.100 & 0.000 \end{bmatrix},$$

$$d_{SrB_4O_7} =$$

$$\begin{bmatrix} -0.025 & 0.025 & 0.000 & 0.000 & -0.004 & -0.458 \\ -0.458 & 0.458 & 0.000 & -0.004 & 0.000 & 0.025 \\ -0.004 & -0.004 & 0.019 & 0.000 & 0.000 & 0.000 \end{bmatrix},$$

$$d_{Al_4(B_2O_5)_3} =$$

$$\begin{bmatrix} 0.388 & -0.388 & 0.000 & 0.000 & 0.648 & 0.018 \\ 0.018 & -0.018 & 0.000 & 0.648 & 0.000 & -0.388 \\ 0.648 & 0.648 & -0.928 & 0.000 & 0.000 & 0.000 \end{bmatrix}.$$

If those results are to be compared with the benchmark of DUV optical crystals – KH_2PO_4 (KDP), that has $d_{36} = 0.38\,\mathrm{pm/V}$, we can then summarize results as follows:

for $K_3B_6O_{10}Cl$:

$$|d_{16}^{K_3B_6O_{10}Cl}| = |d_{21}^{K_3B_6O_{10}Cl}| =$$

$$= |d_{22}^{K_3B_6O_{10}Cl}| = 2.42 \times \mathrm{KDP},$$

$$|d_{33}^{K_3B_6O_{10}Cl}| = 1.15 \times \mathrm{KDP},$$

for $Ca_5B_3O_9F$:

$$|d_{12}^{Ca_5B_3O_9F}| = |d_{26}^{Ca_5B_3O_9F}| = 1.84 \times \mathrm{KDP},$$

$$|d_{15}^{Ca_5B_3O_9F}| = |d_{31}^{Ca_5B_3O_9F}| = 1.25 \times \mathrm{KDP},$$

$$|d_{24}^{Ca_5B_3O_9F}| = |d_{32}^{Ca_5B_3O_9F}| = 1.33 \times \mathrm{KDP},$$

for SrB_4O_7:

$$|d_{16}^{SrB_4O_7}| = |d_{21}^{SrB_4O_7}| = |d_{22}^{SrB_4O_7}| = 20 \times \mathrm{KDP},$$

and for $Al_4(B_2O_5)_3$:

$$|d_{33}^{Al_4(B_2O_5)_3}| = 2.441.70 \times \mathrm{KDP},$$

$$|d_{15}^{Al_4(B_2O_5)_3}| = |d_{31}^{Al_4(B_2O_5)_3}| = |d_{32}^{Al_4(B_2O_5)_3}| = 1.70 \times \mathrm{KDP},$$

$$|d_{11}^{Al_4(B_2O_5)_3}| = |d_{12}^{Al_4(B_2O_5)_3}| = |d_{26}^{Al_4(B_2O_5)_3}| = 1.02 \times \mathrm{KDP}.$$

Conclusions. In summary, we performed the search for promising nonlinear optical materials by screening the Materials Project database and The Open Quantum Materials Database for borate crystals. Among them, we have chosen non-centrosymmetric, thermodynamically stable and low-energy metastable structures, with expected band gap values more than 6 eV, and not deeply studied before. For the collected and pre-filtered structures, the band gaps, birefringence, absorption edge and PM wavelength and non-linear susceptibilities were calculated within the framework of DFT. The resulting promising borate crystals are $K_3B_6O_{10}Cl$, $Ca_5B_3O_9F$, SrB_4O_7, and $Al_4(B_2O_5)_3$.

The findings of this study highlight the critical importance and urgency of leveraging structure prediction algorithms to enhance databases with novel, stable, and low-energy metastable materials. Serving the goal of accelerating the discovery of innovative and promising materials, particularly in the field of nonlinear optics.

Here, we identified four promising borate NLO materials by screening large databases of inorganic crystal structures. Looking at phosphates, a few more materials may be found, but further discoveries in this field demand a broad application of smart crystal structure prediction algorithms, capable of finding unknown stable compounds and their crystal structures.

Funding. The work was funded by Russian Science Foundation grant # 24-43-00162.

Conflict of interest. The authors of this work declare that they have no conflicts of interest.

1. E. Garmire, Opt. Express **21**, 30532 (2013).
2. S. Solgi, M. J. Tafreshi, and M. S. Ghamsari, Crystallogr. Rep. **64**, 1138 (2019).
3. B. Wu, D. Tang, N. Ye, and C. Chen, Opt. Mater. **5**, 105 (1996).
4. I. N. Ogorodnikov, V. A. Pustovarov, S. A. Yakovlev, L. I. Isaenko, and S. A. Zhurkov, Phys. Solid State **54**, 735 (2012).
5. Y. Sun, Z. Yang, D. Hou, and S. Pan, RSC Adv. **7**, 2804 (2017).
6. R. E. Newnham, *Properties of Materials: Anisotropy, Symmetry, Structure*, Oxford University Press, Oxford (2020).
7. T. T. Tran, H. Yu, J. M. Rondinelli, K. R. Poeppelmeier, and P. S. Halasyamani, Chem. Mater. **28**, 5238 (2016).
8. M. Mutailipu and S. Pan, Angew Chem. Int. Ed. **59**, 20302 (2020).
9. M. Xia, X. Jiang, Z. Lin, and R. Li, J. Am. Chem. Soc. **138**, 14190 (2016).

10. X. Chen, B. Zhang, F. Zhang, Y. Wang, M. Zhang, Z. Yang, K. R. Poeppelmeier, and S. Pan, J. Am. Chem. Soc. **140**, 16311 (2018).
11. S. M. Aksenov, N. V. Chukanov, V. P. Tarasov, D. A. Banaru, S. A. Mackley, A. M. Banaru, S. V. Krivovichev, and P. C. Burns, J. Phys. Chem. Solids **189**, 111944 (2024).
12. M. Mutailipu, M. Zhang, Z. Yang, and S. Pan, Acc. Chem. Res. **52**, 791 (2019).
13. Q. Jing, G. Yang, Z. Chen, X. Dong, and Y. Shi, Inorg. Chem. **57**, 1251 (2018).
14. C. Xie, A. Tudi, and A. R. Oganov, Chem. Commun. **58**, 12491 (2022).
15. R. Bubnova, S. Volkov, B. Albert, and S. Filatov, Crystals **7**, 93 (2017).
16. R. Arun Kumar, J. Chem. **2013**, 154862 (2013).
17. M. Cheng, X. Hou, Z. Yang, and S. Pan, Mater. Chem. Front. **7**, 4683 (2023).
18. P. E. Blöchl, Phys. Rev. B **50**, 17953 (1994).
19. G. Kresse and J. Hafner, Phys. Rev. B **47**, 558 (1993).
20. G. Kresse and D. Joubert, Phys. Rev. B **59**, 1758 (1999).
21. J. P. Perdew, K. Burke, and M. Ernzerhof, Phys. Rev. Lett. **77**, 3865 (1996).
22. A. V. Krukau, O. A. Vydrov, A. F. Izmaylov, and G. E. Scuseria, J. Chem. Phys. **125**, 224106 (2006).
23. M. Gajdoš, K. Hummer, G. Kresse, J. Furthmüller, and F. Bechstedt, Phys. Rev. B **73**, 045112 (2006).
24. C. Aversa and J. E. Sipe, Phys. Rev. B **52**, 14636 (1995).
25. S. N. Rashkeev, W. R. L. Lambrecht, and B. Segall, Phys. Rev. B **57**, 3905 (1998).
26. J. L. P. Hughes and J. E. Sipe Phys. Rev. B: Condensed Matter **53**(16), 10751 (1996).
27. A. Jain, S. P. Ong, G. Hautier, W. Chen, W. D. Richards, S. Dacek, S. Cholia, D. Gunter, D. Skinner, G. Ceder, and K. A. Persson, APL Mater. **1**, 011002 (2013).
28. J. E. Saal, S. Kirklin, M. Aykol, B. Meredig, and C. Wolverton, JOM **65**, 1501 (2013).
29. S. Kirklin, J. E. Saal, B. Meredig, A. Thompson, J. W. Doak, M. Aykol, S. Rühl, and C. Wolverton, Npj Comput Mater **1**, 15010 (2015).
30. H. Wu, S. Pan, K. R. Poeppelmeier, H. Li, D. Jia, Z. Chen, X. Fan, Y. Yang, J. M. Rondinelli, and H. Luo, J. Am. Chem. Soc. **133**, 7786 (2011).
31. J. G. Fletcher, F. P. Glasser, and R. A. Howie, Acta Crystallogr. C: Cryst. Struct. Commun. **47**, 12 (1991).
32. S. Lei, Q. Huang, Y. Zheng, A. Jiang, and C. Chen, Acta Crystallogr. C: Cryst. Struct. Commun. **45**, 1861 (1989).
33. A. D. Vasiliev, A. V. Cherepakhin, and A. I. Zaitsev, Acta Crystallogr. E: Struct. Rep. Online **66**, i48 (2010).
34. A. I. Zaitsev, A. S. Aleksandrovskii, A. V. Zamkov, and A. M. Sysoev, Inorg. Mater. **42**, 1360 (2006).
35. J. Ju, T. Yang, G. Li, F. Liao, Y. Wang, L. You, and J. Lin, Chemistry: A European J. **10**, 3901 (2004).
36. V. Trinquet, F. Naccarato, G. Brunin, G. Petretto, L. Wirtz, G. Hautier, and G.-M. Rignanese, Sci. Data **11**, 757 (2024).